Order online now!

www.rockland.com
tech@rockland.com
+1 484.791.3823

Datasheet for 200-101-379

RFP Antibody

Overview

Description:	Anti-RFP (GOAT) Antibody - 200-101-379
Item No.:	200-101-379
Size:	100 µg
Applications:	WB, EM, FC, IF, IHC, Multiplex
Reactivity:	RFP, rRFP
Host Species:	Goat

Product Details

Background:	Antibodies to RFP (Discosoma spp.) are intended for use in immunological assays including ELISA, western blotting, immunofluorescence, and fluorescence activated cell sorting (FACS).
Synonyms:	goat anti-RFP antibody, DsRed, rDsRed, Discosoma sp. Red Fluorescent Protein, Red fluorescent protein drFP583
Host Species:	Goat
Clonality:	Polyclonal
Format:	IgG

Target Details

Gene Name:	DsRed
Reactivity:	RFP, rRFP
Immunogen Type:	Recombinant Protein
Immunogen:	The immunogen is a Red Fluorescent Protein (RFP) fusion protein corresponding to the full length amino acid sequence (234aa) derived from the mushroom polyp coral Discosoma.

Purity/Specificity:	Anti-RFP (GOAT) is an IgG fraction purified from monospecific antiserum by a multi-step process which includes delipidation, salt fractionation and ion exchange chromatography followed by extensive dialysis against the buffer stated above. Assay by immunoelectrophoresis resulted in a single precipitin arc against anti-Goat Serum and purified and partially purified Red Fluorescent Protein (Discosoma). No reaction was observed against Human, Mouse or Rat serum proteins. Expect reactivity against RFP and its variants: mCherry, tdTomato, mBanana, mOrange, mPlum, mOrange and mStrawberry.
Relevant Links:	• UniProtKB - Q9U6Y8

Application Details

Tested Applications:	WB
Suggested Applications:	EM, FC, IF, IHC, Multiplex (Based on references)
Application Note:	Polyclonal anti-RFP has been tested by and western blot and is designed to detect RFP and its variants. Optimal titers for applications should be determined by the researcher. Expect a band ~27kDa in Western Blot in the appropriate cell lysate or extract.
Assay Dilutions:	All assays should be optimized by the user. Recommended dilutions (if any) may be listed below.
ELISA:	1:2,000 - 1:10,000
IF:	User Optimized
WB:	1:1000-1:10,000

Formulation

Physical State:	Liquid (sterile filtered)
Concentration:	1 mg/mL by UV absorbance at 280 nm
Buffer:	0.02 M Potassium Phosphate, 0.15 M Sodium Chloride, pH 7.2
Preservative:	0.01% (w/v) Sodium Azide
Stabilizer:	None

Shipping & Handling

Shipping Condition:	Dry Ice

Storage Condition:	Store vial at -20° C prior to opening. Aliquot contents and freeze at -20° C or below for extended storage. Avoid cycles of freezing and thawing. Centrifuge product if not completely clear after standing at room temperature. This product is stable for several weeks at 4° C as an undiluted liquid. Dilute only prior to immediate use.
Expiration:	Expiration date is one (1) year from date of receipt.

Images

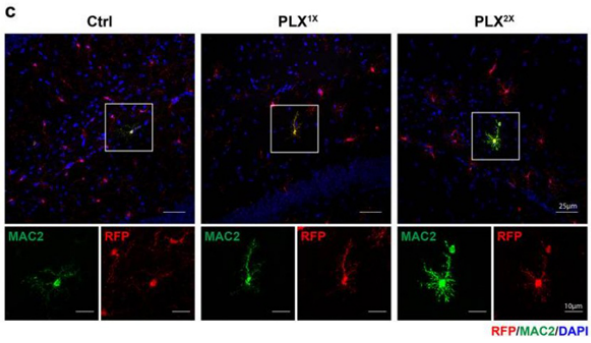

Immunofluorescence Microscopy
(c) Representative confocal images showing colocalization of MAC2 and RFP expression. Boxed area is enlarged and separated by each channel. Images were collected from mouse brain, hippocampal region. Fig 5. PMID: 33054973

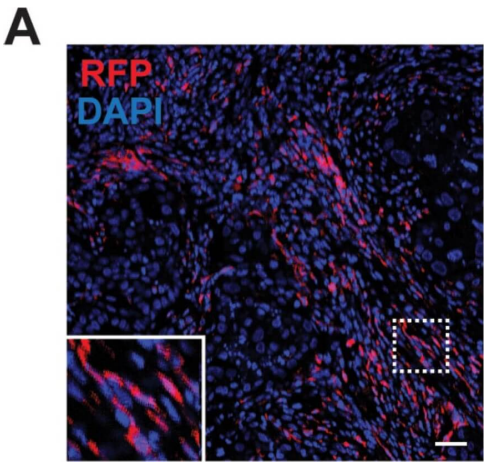

Immunohistochemistry
Population of CD11b + myeloid progenitor cells differentiate into SMA + stromal cells within tumors and in vitro. (A) Representative image of red fluorescent protein (RFP) + stromal cells in tumor from CCR2-RFP heterozygous SCID mouse. (B) RFP + SMA + double positive cells within tumor stroma. (C) CD11b + SMA + double positive cells within tumor stroma. (D) CD45 + CD11b + CD34+ myeloid progenitor cells in the mammary gland at 1.5 (n = 5 empty vector (EV), 7 CCL2) and 2.5 weeks (n = 5 EV, 7 CCL2) post-transplantation were quantified by flow cytometry. (E) CD45 + CD11b + CD34 + myeloid progenitor cells in the bone marrow at 1.5 weeks (n = 6 EV, 7 CCL2) and 2.5 weeks (n = 3 mice/group) post-transplantation were quantified by flow cytometry. (F) Representative brightfield image of colony formed by CD45 + CD11b + CD34 + myeloid progenitor cells isolated using fluorescence-activated cell sorting (FACS). (G) Colonies in culture co-stained with SMA and collagen I. Statistical differences determined by Mann–Whitney U test. Magnification bars = 50 µm. Figure provided by CiteAb. Source: Cancers (Basel), PMID: 32731354.

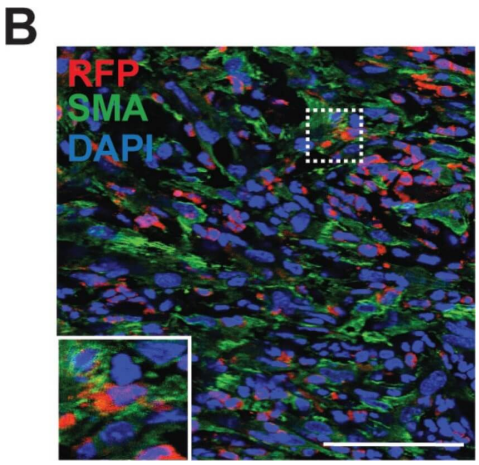

Immunohistochemistry
Population of CD11b + myeloid progenitor cells differentiate into SMA + stromal cells within tumors and in vitro. (A) Representative image of red fluorescent protein (RFP) + stromal cells in tumor from CCR2-RFP heterozygous SCID mouse. (B) RFP + SMA + double positive cells within tumor stroma. (C) CD11b + SMA + double positive cells within tumor stroma. (D) CD45 + CD11b + CD34+ myeloid progenitor cells in the mammary gland at 1.5 (n = 5 empty vector (EV), 7 CCL2) and 2.5 weeks (n = 5 EV, 7 CCL2) post-transplantation were quantified by flow cytometry. (E) CD45 + CD11b + CD34 + myeloid progenitor cells in the bone marrow at 1.5 weeks (n = 6 EV, 7 CCL2) and 2.5 weeks (n = 3 mice/group) post-transplantation were quantified by flow cytometry. (F) Representative brightfield image of colony formed by CD45 + CD11b + CD34 + myeloid progenitor cells isolated using fluorescence-activated cell sorting (FACS). (G) Colonies in culture co-stained with SMA and collagen I. Statistical differences determined by Mann–Whitney U test. Magnification bars = 50 µm. Figure provided by CiteAb.
Source: Cancers (Basel), PMID: 32731354.

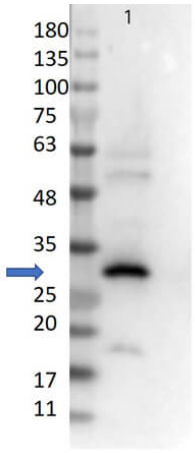

Western Blot
Western Blot of Goat Anti-RFP Antibody. Lane 1: 50ng of RFP protein (p/n 000-001-379). Primary Antibody: Goat Anti-RFP at 1:10,000 overnight at 2-8°C. Secondary Antibody: Donkey anti-Goat IgG HRP (p/n 605-703-125) at 1:40,000 for 30 min at RT. Blocking buffer: BlockOut® (p/n MB-073). Predicted MW: ~27kDa.

References

- Aroca-Crevillén A et al. A circadian checkpoint relocates neutrophils to minimize injury. *J Exp Med.* (2026)
- Alnahrawy E et al. GDF9, NPHS1, and RET Mark Gastric Neuroendocrine Cells and Their Disruption in a PKA-Driven Gastric Preneoplasia Model. *Int J Mol Sci.* (2026)
- Hu, R et al. ERα activates NAMPT/IL-33 signaling to enhance beige thermogenesis and metabolic fitness. *Science Advances* (2026)

- Jin, H et al. Lineage tracing reveals the origins and dynamics of macrophages in lung injury and repair. *Cell Discovery* (2026)
- Zheng, X et al. In vivo multiomic Perturb-seq with enhanced nuclear gRNA capture. *BioRxiv [Preprint]* (2026)
- Ibrahimi, M et al. TRACR: an anterograde transneuronal tracing system for genetic access across synapses and longitudinal circuit analysis. *BioRxiv [Preprint]* (2026)
- Tamura, S et al. Dual targeting of astrocytic and endothelial GLUT1 enables functional rescue in GLUT1 deficiency syndrome. *BioRxiv [Preprint]* (2026)
- Trinchero MF et al. Audiovisual gamma stimulation enhances hippocampal neurogenesis and neural circuit plasticity in aging mice. *bioRxiv [preprint]* (2025)
- Wu Y et al. Multimodal transcriptomics reveal neurogenic aging trajectories and age-related regional inflammation in the dentate gyrus. *Nat Neurosci.* (2025)
- Cortado H et al. Murine Ribonuclease 6 Limits Bacterial Dissemination during Experimental Urinary Tract Infection. *J Innate Immun.* (2024)
- Kumar R et al. Interstitial macrophage phenotypes in Schistosoma-induced pulmonary hypertension. *Front Immunol.* (2024)
- Curran BM et al. Multiple Guidance Mechanisms Control Axon Growth to Generate Precise T-shaped Bifurcation during Dorsal Funiculus Development in the Spinal Cord. *bioRxiv [Preprint].* (2024)
- Cathomas F et al. Circulating myeloid-derived MMP8 in stress susceptibility and depression. *Nature.* (2024)
- Recinto SJ et al. Characterizing enteric neurons in dopamine transporter (DAT)-Cre reporter mice reveals dopaminergic subtypes with dual-transmitter content. *Eur J Neurosci.* (2024)
- Amato Jr E et al. Illuminating the terminal nerve: Uncovering the link between GnRH-1 neuron and olfactory development. *J Comp Neurol.* (2024)
- Haist KC et al. A LTB4/CD11b self-amplifying loop drives pyogranuloma formation in chronic granulomatous disease. *iScience.* (2024)
- Ciceri G et al. An epigenetic barrier sets the timing of human neuronal maturation. *Nature.* (2024)
- Liu K et al. Tracing the origin of alveolar stem cells in lung repair and regeneration. *Cell.* (2024)
- Liu K et al. Intercellular genetic tracing of cardiac endothelium in the developing heart. *Dev Cell.* (2023)
- Ruiz-Rosado, Juan de Dios et al. Human ribonuclease 6 has a protective role during experimental urinary tract infection. *J Innate Immun.* (2023)
- Hayes BH et al. Confinement plus myosin-II suppression maximizes heritable loss of chromosomes, as revealed by live-cell ChReporters. *J Cell Sci.* (2023)
- Deng L et al. Nav1.7 is essential for nociceptor action potentials in the mouse in a manner independent of endogenous opioids. *Neuron.* (2023)
- Pu W et a. Bipotent transitional liver progenitor cells contribute to liver regeneration. *Nat Genet* (2023)
- Wang J et al. An ultra-compact promoter drives widespread neuronal expression in mouse and monkey brains. *Cell Rep.* (2023)

- Liu L et al. Modeling post-implantation stages of human development into early organogenesis with stem-cell-derived peri-gastruloids. *Cell.* (2023)
- Lauer SM et al. Recruitment of BAG2 to DNAJ-PKAc scaffolds promotes cell survival and resistance to drug-induced apoptosis in fibrolamellar carcinoma. *bioRxiv [Preprint].* (2023)
- Noack F et al. Joint epigenome profiling reveals cell-type-specific gene regulatory programmes in human cortical organoids. *Nat Cell Biol.* (2023)
- Rashid M et al. Inhibition of high-fat diet-induced inflammatory responses in adipose tissue by SF1-expressing neurons of the ventromedial hypothalamus. *Cell Rep,* (2023)
- Masuda T et al. Pancreatic RECK inactivation promotes cancer formation, epithelial-mesenchymal transition, and metastasis. *J Clin Invest.* (2023)
- Nam HS et al. Lrig1 expression identifies quiescent stem cells in the ventricular□subventricular zone from postnatal development to adulthood and limits their persistent hyperproliferation. *Neural Dev.* (2023)
- Zhao H et al Use of a dual genetic system to decipher exocrine cell fate conversions in the adult pancreas. *Cell Discov.* (2023)
- Ota R et al. Cortical projection to the subventricular zone and its effect on adult neurogenesis in mice. *Neurosci Lett.* (2023)
- Salery M et al. Transcriptional correlates of cocaine-associated learning in striatal ARC ensembles. *bioRxiv [Preprint].* (2023)
- Sato Y et al. Aquaporin regulates cell rounding through vacuole formation during endothelial-to-hematopoietic transition. *Development.* (2023)
- Chen APF et al. Nigrostriatal dopamine modulates the striatal-amygdala pathway in auditory fear conditioning. *Nat Commun.* (2023)
- Szabo GG et al. Ripple-selective GABAergic projection cells in the hippocampus. *Neuron.* (2022)
- Ademi H et al. Deciphering the origins and fates of steroidogenic lineages in the mouse testis. *Cell Rep.* (2022)
- Le N et al. Ectopic insert-dependent neuronal expression of GFAP promoter-driven AAV constructs in adult mouse retina. *Front Cell Dev Biol.* (2022)
- Yao L et al. Temporal control of PDGFRα regulates the fibroblast-to-myofibroblast transition in wound healing. *Cell Rep.* (2022)
- Puri P et al. Elevated Protein Kinase A Activity in Stomach Mesenchyme Disrupts Mesenchymal-epithelial Crosstalk and Induces Preneoplasia. *Cell Mol Gastroenterol Hepatol.* (2022)
- Hou WH et al. Inhibitory Fear Memory Engram in the Mouse Central Lateral Amygdala. *Cell Press Preprint* (2022)
- Weera, MM et al. Generation of a CRF1-Cre transgenic rat and the role of central amygdala CRF1 cells in nociception and anxiety-like behavior. *ELife* (2022)
- Topilko, T et al. Edinger-Westphal peptidergic neurons enable maternal preparatory nesting. *Neuron* (2022)
- Serrano, J et al. Saccharin Stimulates Insulin Secretion Dependent on Sweet Taste Receptor-Induced Activation of PLC Signaling Axis. *Biomedicines* (2022)

- Serrano J et al. Saccharin Stimulates Insulin Secretion Dependent on Sweet Taste Receptor-Induced Activation of PLC Signaling Axis. *Biomedicines.* (2022)
- Maksymetz J et al. mGlu1 potentiation enhances prelimbic somatostatin interneuron activity to rescue schizophrenia-like physiological and cognitive deficits. *Cell Rep.* (2021)
- Delpech JC et al. Wolframin-1–expressing neurons in the entorhinal cortex propagate tau to CA1 neurons and impair hippocampal memory in mice. *Sci Transl Med.* (2021)
- Weera MM et al. Generation and validation of a CRF1:Cre transgenic rat: The role of central amygdala CRF1 in nociception and anxiety-like behavior. *bioRxiv Preprint* (2021)
- Treffy RW et al. Neuroblastoma differentiation in vivo excludes cranial tumors. *Dev Cell.* (2021)
- Yao L et al. Fibrosis Without Myofibroblasts Revealed by Genetic Analysis of PDGFRα. *Cell Press Preprint* (2021)
- Haidey JN et al. Astrocytes regulate ultra-slow arteriole oscillations via stretch-mediated TRPV4-COX-1 feedback. *Cell Rep.* (2021)
- Mayere C et al. Origin, specification and differentiation of a rare supporting-like lineage in the developing mouse gonad. *HAL Preprint.* (2021)
- Holt JR et al. Spatiotemporal dynamics of PIEZO1 localization controls keratinocyte migration during wound healing. *Elife.* (2021)
- Ishikura Y et al. In vitro reconstitution of the whole male germ-cell development from mouse pluripotent stem cells. *Cell Stem Cell.* (2021)
- Okuchi Y et al. Wnt-modified materials mediate asymmetric stem cell division to direct human osteogenic tissue formation for bone repair. *Nat Mater.* (2021)
- Junyent S et al. Pluripotency state regulates cytoneme selectivity and self-organization of embryonic stem cells. *J Cell Biol.* (2021)
- Zhang W et al. Targeting KDM4A epigenetically activates tumor-cell-intrinsic immunity by inducing DNA replication stress. *Mol Cell.* (2021)
- Hara A et al. Meflin defines mesenchymal stem cells and/or their early progenitors with multilineage differentiation capacity. *Genes Cells.* (2021)
- Kuziel G, Thompson V, D'Amato JV, Arendt LM. Stromal CCL2 Signaling Promotes Mammary Tumor Fibrosis through Recruitment of Myeloid-Lineage Cells. *Cancers (Basel).* (2020)
- Kim CK, Saxena M, Maharjan K, et al. Krüppel-like Factor 5 Regulates Stemness, Lineage Specification, and Regeneration of Intestinal Epithelial Stem Cells. *Cell Mol Gastroenterol Hepatol.* (2020)
- Uchigashima M. et al. A Specific Neuroligin3-αNeurexin1 Code Regulates GABAergic Synaptic Function in Mouse Hippocampus. *ELife* (2020)
- Turi GF, Li WK, Chavlis S, et al. Vasoactive Intestinal Polypeptide-Expressing Interneurons in the Hippocampus Support Goal-Oriented Spatial Learning. *Neuron.* (2019)
- Lihong Zhan et al. A Mac2-positive progenitor-like microglial population survives independent of CSF1R signaling in adult mouse brain. *Elife.* (2019)

- Chen M, Reed RR, Lane AP. Acute inflammation regulates neuroregeneration through the NF-κB pathway in olfactory epithelium. *Proc Natl Acad Sci U S A.* (2017)
- Lebrigand, K et al. Comparative Genomic Analysis of Drechmeria coniospora Reveals Core and Specific Genetic Requirements for Fungal Endoparasitism of Nematodes. *PloS Genetics* (2016)
- Clancy, JW et al. Regulated delivery of molecular cargo to invasive tumour-derived microvesicles. *Nature Communications* (2015)

Disclaimer